CrystEngComm

An organometallic complex revealing an unexpected, reversible, temperature induced SC-SC transformation

Journal:	*CrystEngComm*
Manuscript ID:	CE-ART-01-2014-000070.R2
Article Type:	Paper
Date Submitted by the Author:	26-Mar-2014
Complete List of Authors:	Pope, Simon; University of Cardiff, School of Chemistry Taylor, Rupert; Cardiff University, Yeo, Benjamin; Cardiff University, Hallett, Andrew; Cardiff University, Chemistry Kariuki, Benson; Cardiff University, Chemistry

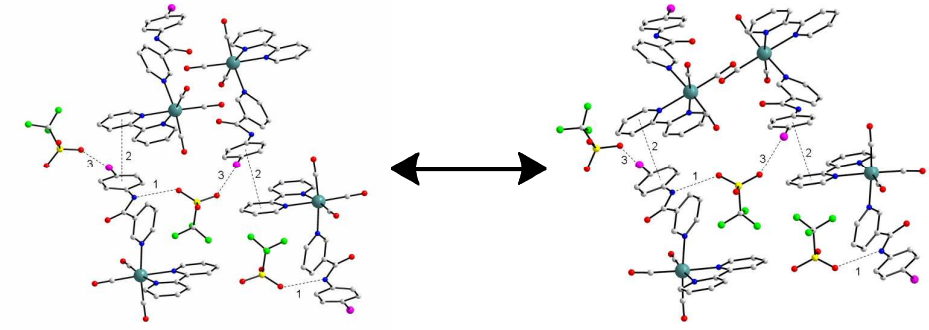

SC-SC transformation at ca. 180 K

Cite this: DOI: 10.1039/c0xx00000x

www.rsc.org/xxxxxx

ARTICLE TYPE

An organometallic complex revealing an unexpected, reversible, temperature induced SC-SC transformation

Rupert G.D. Taylor,[a] Benjamin R. Yeo,[a] Andrew J. Hallett,[a] Benson M. Kariuki,*[a] Simon J.A. Pope*[a]

Received (in XXX, XXX) Xth XXXXXXXXX 20XX, Accepted Xth XXXXXXXXX 20XX

DOI: 10.1039/b000000x

A reversible, temperature driven phase transformation that takes place at *ca.* 180K, in a single-crystal to single-crystal manner, has been observed for a monometallic transition metal coordination complex based on a *fac*-Re(CO)$_3$ core, with a chelated 2,2′-bipyridine unit and a halogenated N-(4-iodophenyl)nicotinamide axial co-ligand. A range of closely related analogues that varied the halogen and its position of substitution exemplified the rarity of such an observation: none of the eight structurally related examples demonstrated such interesting behavior in the temperature range of study. The structures of all the complexes also revealed that the trifluoromethanesulfonate counter anion plays an important role through hydrogen bonding, but no isomorphism or polymorphism was observed. The latter are also fully characterised from a spectroscopic perspective, with IR, UV-vis., time-resolved luminescence and NMR spectroscopies providing complementary solution-state data.

Introduction

Transformations in the solid state are associated with a variety of processes, including elimination or incorporation of guest molecules, solid-state chemical reactions, and transitions between polymorphs. In the crystalline state, chemical reactions are generally highly specific and efficient. This specificity and efficiency can be rationalised on the basis of the topochemical principal, developed several decades ago through the study of reactions in the solid state of organic substances, and specifically the photochemistry of the cinnamic acids.[1] In addition to application in clean solvent-free synthesis, solid state reactions are also potential synthetic routes to new materials that are inaccessible by conventional solution methods.[2]

On rare occasions, transformation can proceed without compromising crystal integrity *i.e.* in a single-crystal to single-crystal (SC-SC) manner. This retention of three-dimensional order often requires the structural difference between the initial and final states to be small, and any steric barrier during the process to be low. SC-SC processes continue to draw interest because they can provide information about reaction mechanisms. There has been a recent upsurge in the interest in SC-SC processes in metal-organic compounds[3] with reports of processes driven by a variety of methods, including thermal[3a,i,p], photochemical[3g], mechanochemical[3a] treatment, exposure to vacuum[3l] conditions, and to gases[3b,o] as well as soaking[3c,e,h] in solvents or solutions. The reported examples have predominantly involved incorporation or expulsion of reagents and products into, or out of the crystal, including processes such as solvation and desolvation,[3l,d,j] ligand and solvent exchange[3b,m,k] as well as cation exchange.[3c,o].

Polymorphic phase transformation is not accompanied by a change in the chemical composition or bonding and is the result of a switch in the relative thermodynamic stabilities of the polymorphs. The switch may be driven by a number of factors, including changes in temperature and pressure as well as mechanical treatment, and can often be accompanied by the loss of single crystallinity. Polymorphic phase transformation represents a special situation where the delicate balance between interactions within the crystal can be perturbed by a relatively small change in environmental conditions, and therefore provides an opportunity to obtain some insight into the subtle interplay between intra-crystalline interactions.[4]

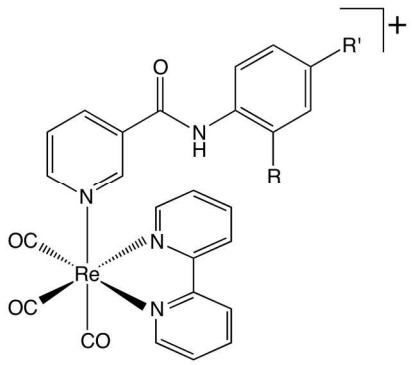

Scheme 1 General structure of the halogenated rhenium complexes: **Re-*p*-F** R = H, R′ = F; **Re-*o*-F** R= F, R′ = H; **Re-*p*-Cl** R = H, R′ = Cl; **Re-*o*-Cl** R= Cl, R′ = H; **Re-*p*-Br** R = H, R′ = Br; **Re-*o*-Br** R= Br, R′ = H; **Re-*p*-I** R = H, R′ = I; **Re-*o*-I** R= I, R′ = H.

During our routine structural characterisation of a luminescent organometallic rhenium (I) ligand complex, it was discovered that this species (designated **Re-*p*-I**) displayed a very rare and remarkable thermal phase transformation, occurring in a SC-SC

manner. The discovery of the transformation was particularly interesting because polymorphism can be a route to materials with different physical properties for a given molecular composition,[5] as illustrated by the different UV-vis. absorption and emission properties of the two polymorphs of [$Re_2(\mu$-$Cl)_2(CO)_6(\mu$-4,5-$(Me_3Si)_2$pyridazine)].[3r]

As phase transformations are the result of subtle shifts in the balance of molecular interactions, one approach to investigating such phenomena would be to introduce structural modifications to a system that demonstrates such a phase transformation. Therefore this paper focuses on the synthesis and characterization of a systematic series of structural analogues (Scheme 1) of **Re-*p*-I** with the potential to display comparable structural and thermal properties. The outcome of this study revealed that despite this methodological rationale, no isomorphism or additional phase transformations were discovered for the structural variants. The investigation is therefore instructive as it highlights the inherent challenges associated with engineering crystalline materials with specific structural and physical properties. The paper firstly describes the synthesis and structural characterisation of the complete series of rhenium complexes and subsequently focuses on the unique SC-SC transformation of the anomolous complex, **Re-*p*-I**.

Results and Discussion

The systematic study on a series of closely related complex derivatives was initiated in an attempt to elucidate any trends in physical behaviour to the structures. The aim was to generate isomorphous structures by exploitation of halogen-halogen similarity[14] and methyl-halogen interchangeability[15] to explore the effect of sterics, polarisability and electronic properties of the ligand substituent on the thermal behaviour of the solid material.

Ligands based on the substituted phenylnicotinamide were prepared, namely, 2-fluoro, 2-bromo, 2-iodo, 4-flouro, 4-chloro, 4-bromo and 4-methyl derivatives (Scheme 1) and the corresponding *fac*-$[Re(CO)_3bipy(L)]^+$ complexes synthesised. For consistency, the same counter-anion was retained throughout and the recrystallisation method was generally performed at room temperature using the same solvent/anti-solvent combinations (acetonitrile/diethyl ether). The exception was the methyl-derivative, for which additional solvents were attempted, as discussed later.

The nicotinamide-derived ligands were easily obtained by reacting an excess (*ca.* 2 eq.) of freshly isolated nicotinoyl chloride with a range of 2- (*ortho*) and 4-substituted (*para*) aniline derivatives. Purification was achieved by repeated extraction of the crude reaction mixture with water thereby removing unreacted nicotinoyl chloride as nicotinic acid. The ligands (labeled ***o*-X** and ***p*-X** for the *ortho*- and *para*-substituted species) were coordinated to rhenium using the convenient precursor *fac*-$[Re(CO)_3bipy(MeCN)](OTf)$ and chloroform (at reflux) as solvent. Typically reactions were completed within 24 hours.[16] The resultant complexes *fac*-$[Re(CO)_3bipy(L)](OTf)$ are abbreviated to **Re-*o*-X** or **Re-*p*-X** in the subsequent discussions.

Spectroscopic characterisation of the complexes

The complexes were characterised in the solution state using a variety of spectroscopies. IR spectroscopy confirmed the geometric arrangement of the carbonyl groups at rhenium (Table 1): typically two stretches were observed at around 2030 and 1920 cm^{-1}, consistent with a pseudo C_{3v} local symmetry at rhenium. An additional lower energy carbonyl stretch (*ca.* 1700 cm^{-1}) was observed that corresponds to the presence of the amide carbonyl within the axial ligand. ^{1}H NMR spectroscopic studies ($CDCl_3$) confirmed the 1:1 stoichiometric formulation of the complexes whilst revealing a downfield shift of the proton resonances associated with the pyridine moiety upon complexation with rhenium. The integrities of the complexes were also established using LR and HR MS methods, each confirming the presence of the cationic complex moiety and the $^{185/187}$Re isotopic distribution of the complexes.

The electronic properties of the complexes (Table 1) were assessed in chloroform solution and revealed characteristic features common to this class of complex. The pale yellow colour of the complexes can be attributed to a $^1M_{Re}L_{bpy}CT$ transition that broadly absorbs around 330 nm, tailing to 400 nm. Ligand-centred absorptions dominate to higher energy (< 320 nm) with $^1\pi$-π^* contributions from both the 2,2′-bipyridine and the aryl axial ligand. Each of the complexes possessed classical ^{3}MLCT emission: a broad, featureless emission dominating at around 539-549 nm, with only very minor differences observed through structural variations of the axial ligand.[17] The corresponding luminescence lifetimes confirmed the phosphorescent nature of the emission, typical of cationic complexes of this type.[16a,16g] The lifetime data suggest that the presence of the heavier halide atoms in the axial nicotinamide does not impart any excited state quenching.

Table 1. IR, UV-vis. and luminescence spectroscopic data for the complexes.

Compound	C≡O ν /cm^{-1} [a]	^{1}MLCT λ_{abs} /nm [b]	^{3}MLCT λ_{em} /nm [c]	τ /ns [d]
Re-*p*-F	2026, 1928	396 sh	549	324
Re-*o*-F	2026, 1928	358 sh	542	361
Re-*p*-Cl	2037, 1933	365 sh	538	321
Re-*o*-Cl	2038, 1933	392 sh	548	333
Re-*p*-Br	2037, 1933	363 sh	542	359
Re-*o*-Br	2037, 1929	358 sh	542	351
Re-*p*-I	2037, 1933	369 sh	545	348
Re-*o*-I	2026, 1900	370 sh	542	334
Re-*p*-Me	2036, 1939	362 sh	543	339

[a] solid; [b] $CHCl_3$; [c] $CHCl_3$, λ_{em} = 370 nm; [d] $CHCl_3$, λ_{em} = 295 nm.

Structural characterisation of the ligands

A number of ligands yielded crystals (Fig S1, ESI) suitable for crystal structure determination during the course of the study and the structures are presented in the ESI. Selected crystallographic data are presented in Table S1 ESI.

The structures suggest a tendency towards planarity accompanied by pyridyl ring participation in hydrogen bonding of the *p*-substituted ligands. Unsurprisingly, the *o*-substituted ligands are less planar due to steric effects and favour hydrogen bonding between amide groups.

Structural characterisation of the complexes

As the purpose of the discussion is to compare the general characteristics of a range of structures, the following analysis is restricted mainly to conformational, hydrogen bonding and π-π interaction properties, rather than a detailed description of each structure.

The *para*-substituted complexes, Re-*p*-X

Selected crystallographic data are presented in Table 2. The Re^{I} coordination geometry in the monoclinic structure of **Re-*p*-F** (Fig. 1a) is distorted octahedral. Pairs of triflate anions occupy pockets in the structure with each triflate anion accepting one N-H···O hydrogen bond (labelled *1* in Fig. 1b) from the ligand amide group, with distances H···O = 2.11Å, N…O = 2.96(2) Å, N–H···O = 161.1°). The *N*-(4-fluorophenyl)nicotinamide ligand is almost planar with an angle of 8.6° between the planes of the fluorophenyl and pyridyl groups. In the structure, π-π type interactions occur between the fluorophenyl rings and the bipyridyl rings of neighbouring cations (labelled *2* in Fig. 1b, with a centroid-to-centroid separation of 3.70(2) Å) to form chains parallel to the *a*-axis.

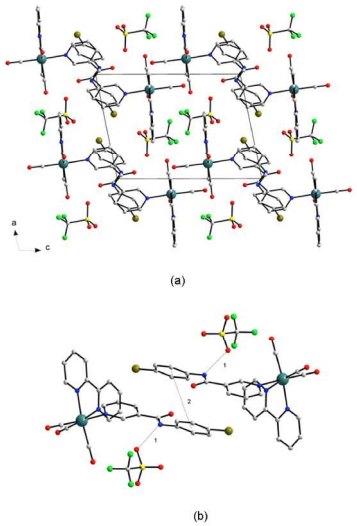

Fig. 1 (a) The structure of the 4-fluoro complex, **Re-*p*-F**, and (b) a segment of the structure.

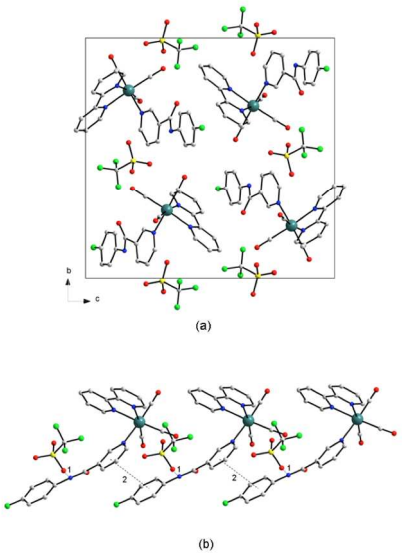

Fig. 2 (a) The structure of the 4-choro complex, **Re-*p*-Cl**, and (b) a segment of the structure.

The triclinic structure of **Re-*p*-Cl** (Fig. 2) also has distorted octahedral coordination geometry for Re^{I}. In the structure, triflate anions also occur in pairs, with each anion accepting one N-H···O hydrogen bond (labelled *1* in Fig. 2b) with distances H···O = 2.10Å, N···O = 2.88(2) Å, and angle N–H···O = 147.3°). In the *N*-(4-chlorophenyl)nicotinamide ligand the angle between the planes of chlorophenyl and pyridyl groups is 40.2(9)°. Some π-π interaction is observed between the bipyridyl rings of neighbouring cations (centroid-centroid separation of 4.04(2) Å), but the closest centroid-centroid contact between the chlorophenyl rings is 4.30(2) Å (labelled *2* in Fig. 2b), with minimal ring overlap.

The crystal structure of **Re-*p*-Br** (Fig. 3a) is monoclinic and contains two crystallographically unique complex cations and two triflate counterions. The angles between the planes of bromophenyl and pyridyl groups in the two independent *N*-(4-bromophenyl)nicotinamide ligands are 50.5(6)° and 58.2(6)°. Triflate anions are accommodated in pairs within the crystal structure, with each ion accepting one amide hydrogen bond. The bonds are labelled *1a* (H1···O10 = 2.18Å, N1···O10 = 2.99(1) Å, N–H···O = 152.1°) and *1b* (H5a···O12 = 2.13Å, N5···O12 = 2.96(1) Å, N–H···O = 157.8°) in Fig. 3b. The closest π-π contact (labelled *2* in Fig. 3b) involves two independent bromophenyl rings, which are not parallel (the inter-planar angle is 26.6(6)°) and have a centroid-to-centroid distance of 4.23(1) Å.

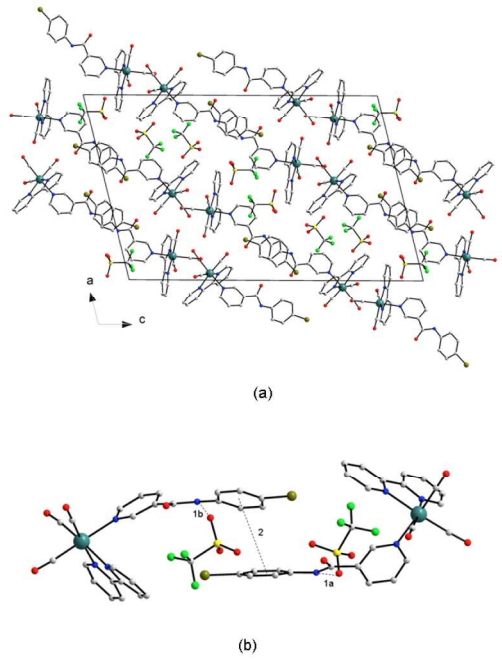

Fig. 3 (a) The structure of the 4-bromo complex, **Re-*p*-Br**, and (b) a segment of the structure.

Unlike the other structures of complexes presented in this study, the crystals of the 4-methyl derivative, **Re-*p*-Me**, were obtained only in solvated form. Initial recrystallisation using the standard conditions (room temperature and acetonitrile/diethyl ether) produced **Re-*p*-Me-A**. Subsequent attempts using other solvents did not produce usable crystals except for a second solvated form, **Re-*p*-Me-B**, from chloroform/diethyl ether. For **Re-*p*-Me-A** (Fig. 4a) the crystal structure is monoclinic and contains two crystallographically unique complex cations and two triflate ions.

The conformations of the *N*-(4-methylphenyl)nicotinamide ligands in the two independent complex units are similar, as evidenced by the angles between the planes of methylphenyl and pyridyl groups (25.(2)° and 26.(2)°). The structure contains ordered acetonitrile solvent molecules, which, together with the anions and cations, create channels around sites occupied by disordered water molecules as well as voids in which no solvent has been located. The two independent triflate anions are isolated from each other, with just one participating in hydrogen bonding (Fig. 4b). The anion accepts two N-H···O hydrogen bonds from amide groups of ligands of two neighbouring independent cations; the hydrogen bonds are labelled *1a* (H1···O9 = 2.12Å, N1···O9 = 2.97(2) Å, N1–H1···O9 = 162.4°) and *1b* (H5a···O10 = 2.23Å, N5···O10 = 3.08(2) Å, N5–H5a···O10 = 162°) in Fig. 4b. The planes of the two ligands hydrogen bonded to one triflate are roughly parallel to each other, with ring centroid separations of 3.63(2)Å and 3.72(2) Å (labelled *2a* and *2b*, respectively, in Fig. 4b).

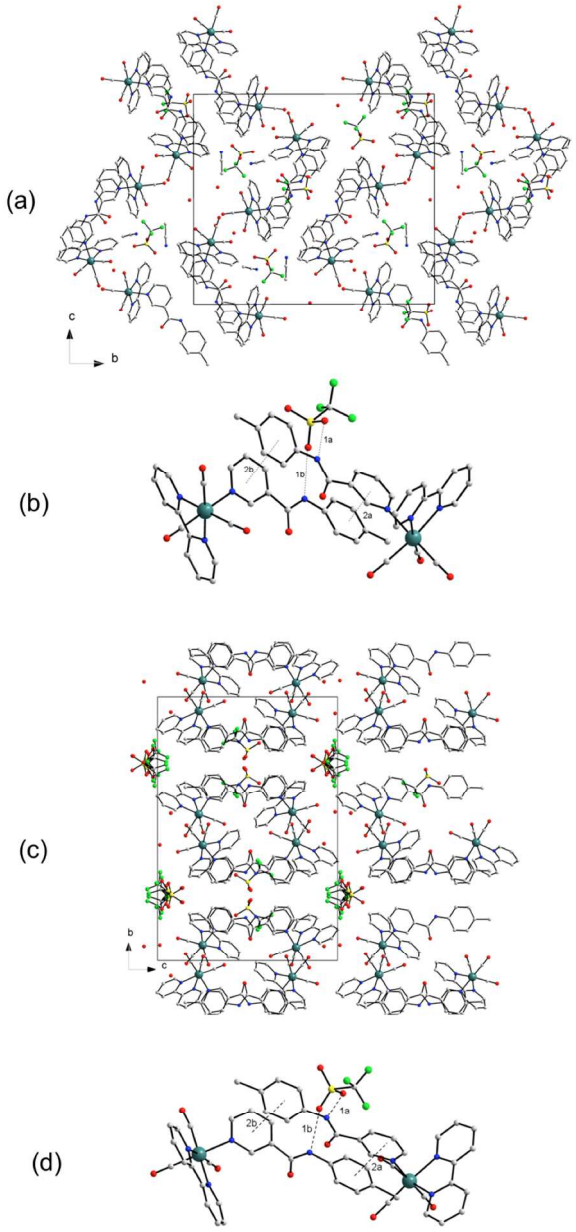

Fig. 4 (a) Crystal packing in the 4-methyl substituted complex (**Re-*p*-Me-A**) and (b) a segment of the structure. (c) Crystal packing in 4-methyl substituted complex (**Re-*p*-Me-B)** and (d) a segment of the structure. Hydrogen atoms have been omitted for clarity.

The second solvate, **Re-*p*-Me-B** (Fig. 4c) is also monoclinic and contains two crystallographically unique complex cations and two triflate ions. The conformations of the two independent *N*-(4-methylphenyl)nicotinamide ligands in the complex units are also fairly similar, with angles of 26(1)° and 24(1)° between the planes of methylphenyl and pyridyl groups. In a similar manner to **Re-*p*-Me-A**, the two triflate anions are isolated from each other, with just one participating in hydrogen bonding (Fig. 4d)

by accepting two N-H···O hydrogen bonds from two independent ligands - labelled *1a* (H1···O9 = 2.05Å, N1···O9 = 2.90(4) Å, N1–H1···O9 = 162°) and *1b* (H5a···O11 = 2.22Å, N5···O11 = 3.02(4) Å, N5–H5a···O11 = 151°) in Fig. 4d. The two ligands involved in hydrogen bonding to one triflate are also roughly parallel to each other, with ring centroid separations of 3.71(4)Å and 3.61(4) Å (labelled *2a* and *2b*, respectively, in Fig. 4d).

The structure can be visualised as consisting of two types of channels running parallel to the *a*-axis (Fig. 4a) with one type occupied by disordered water molecules and the other type by the second triflate ion which is not involved in hydrogen bonding. The second triflate occupies a site displaying two-fold disorder (occupancy: 0.59/0.41), in contrast to **Re-*p*-Me-A** in which both anions are ordered.

The crystals structures **Re-*p*-Me-A** and **Re-*p*-Me-B** both contain the same number of ions and cations and consist of channels. However, they are not polymorphs in the true sense because they incorporate additional solvent and/or water molecules in different proportions. Despite the differences in solvent incorporation, both structures contain a common motif involving one triflate anion and two complex cations (Fig. 4b and c), indicating that the hydrogen bonding, π-π, electrostatic and other interactions involved generate a robust unit.

The *ortho*-substituted complexes, Re-*o*-X

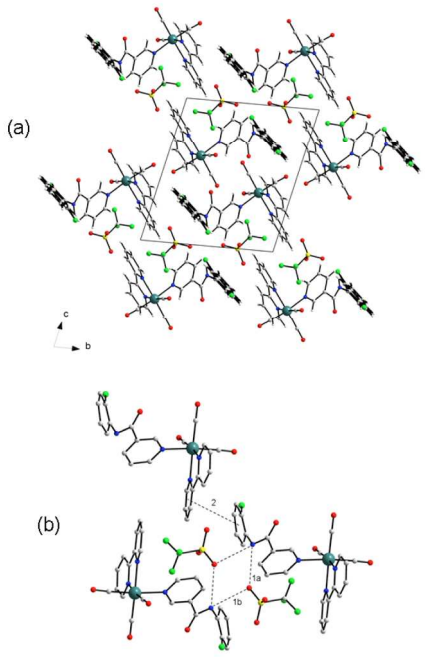

Fig. 5 (a) Crystal packing in the 2-fluoro substituted complex (Re-*o*-F) and (b) a segment of the structure. Hydrogen atoms have been omitted for clarity.

Selected crystallographic data are presented in Table 2. The crystal structure of **Re-*o*-F** (Fig. 5a) is triclinic, with the 2-fluorophenyl group of the the *N*-(2-fluorophenyl)nicotinamide ligand showing disorder between two orientations (0.83/0.17 occupancy) related roughly by a two-fold rotation about the N-C bond. For the major component, the angle between the planes of fluorophenyl and pyridyl groups is 76.24°. Pairs of triflate anions occupy pockets in the structure and one O atom of every triflate ion accepts two amide N-H···O hydrogen bonds from ligands of two complexes. Each ligand is involved in bifurcated hydrogen bonding as shown in Fig. 5b (labelled *1a* (H···O = 2.29Å, N···O = 3.01(1) Å, N–H···O = 139.7°) and *1b* (H···O = 2.56Å, N···O = 3.25(1) Å, and angle N–H···O = 136.1°). The closest π-π contact involves nonparallel fluorophenyl and bipyridyl rings separated by a centroid-to-centroid distance of 3.96(2) Å (labelled *2* in Fig. 5b) with an interplanar angle of 25.1(9)°.

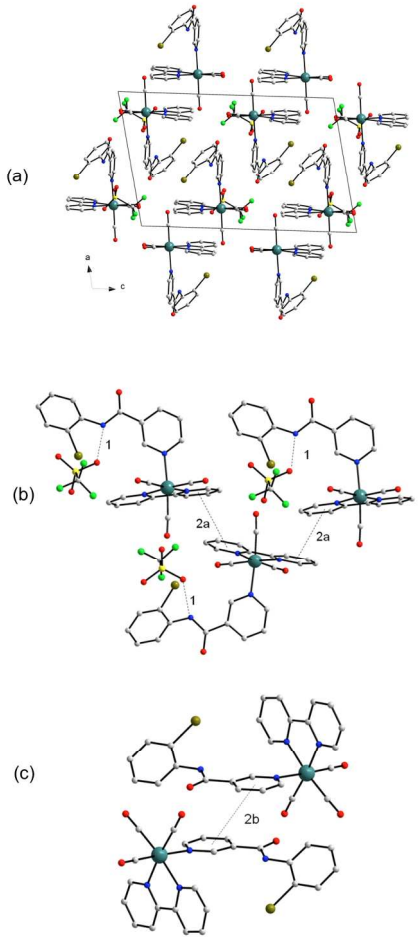

Fig. 6 (a) Crystal packing in the 2-bromo substituted complex (**Re-*o*-Br**) and (b), (c) segments of the structure. Hydrogen atoms have been omitted for clarity.

The **Re-*o*-Br** crystal structure (Fig. 6a) is monoclinic. The angle between the planes of bromophenyl and pyridyl groups in the *N*-(2-bromophenyl)nicotinamide ligand is 46.3(7)°. Pairs of triflate ions occupy spaces in the structure and just one triflate O atom is involved in N-H···O hydrogen bonding (labelled *1* in Fig. 6b), H···O = 2.21Å, N···O = 2.87(1) Å, N–H···O = 131.4°). The closest π-π contact involves non-parallel bipyridine rings separated by a centroid-to-centroid distance of 4.21(2) Å (labelled *2a* in Fig. 6b) with an interplanar angle of 18.1(7)°. The contact between pyridyl rings is longer (4.46(2) Å, labelled *2b* in Fig. 6c).

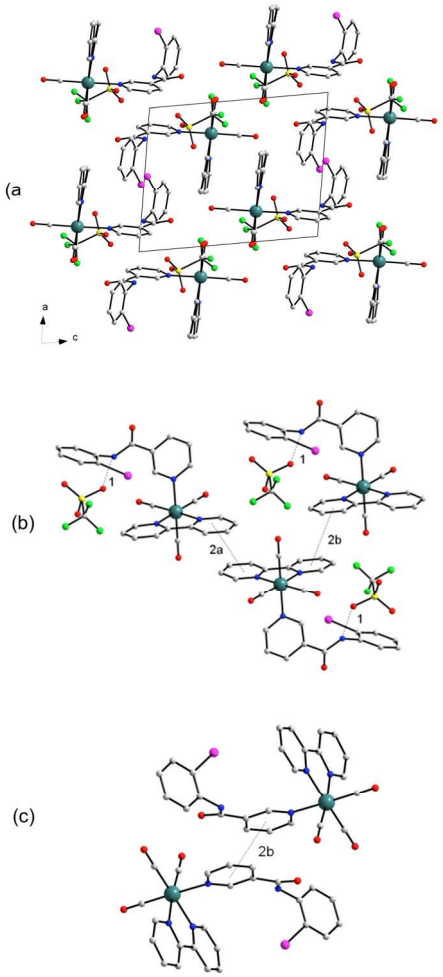

Fig. 7 (a) Crystal packing in the 2-iodo substituted complex (**Re-*o*-I**) and (b), (c) segments of the structure. Hydrogen atoms have been omitted for clarity.

The structure of the iodo- analogue, Re-*o*-I, is triclinic (Fig. 7a). The angle between the planes of iodophenyl and pyridyl groups in the *N*-(2-iodophenyl)nicotinamide ligand is 87.9(5)°. Unlike in the structure of Re-*o*-Br, individual triflate ions are isolated from each other and just one triflate O atom is involved in N-H···O hydrogen bonding (labelled *1* in Fig. 7b, H···O = 2.05Å, N···O = 2.91(1) Å, N–H···O = 162.5°). Contacts of π-π type are observed between the bipyridine rings of neighbouring units with centroid-to-centroid separation distances of 3.89(1) Å (labelled *2a* in Fig. 8b) and 4.44(1) Å (labeled *2b* in Fig. 7b). The closest contact between *N*-(2-iodophenyl)nicotinamide ligands involves pyridyl rings with a distance of 4.49(1) Å (labelled *2b* in Fig. 7c). Crystal packing in Re-*o*-Br (Fig. 6a) and Re-*o*-I (Fig. 7a) indicates that the chloro and bromo substituents are not directly interchangeable in these complexes although local similarities do exist, as illustrated in Figs. 6b,c and 7b,c.

Structural characterisation of Re-*p*-I

During the structural characterisation of the 4-iodo-substituted complex, **Re-*p*-I**, different unit cells were obtained at 294K and 105K and full diffraction data were collected at these temperatures in order to determine the crystal structures of the high temperature (**Re-*p*-I-HT**) and low temperature forms (**Re-*p*-I-LT**) of the complex. Both crystal structures are monoclinic forms of **Re-*p*-I**. Selected crystallographic data are presented in Table 2.

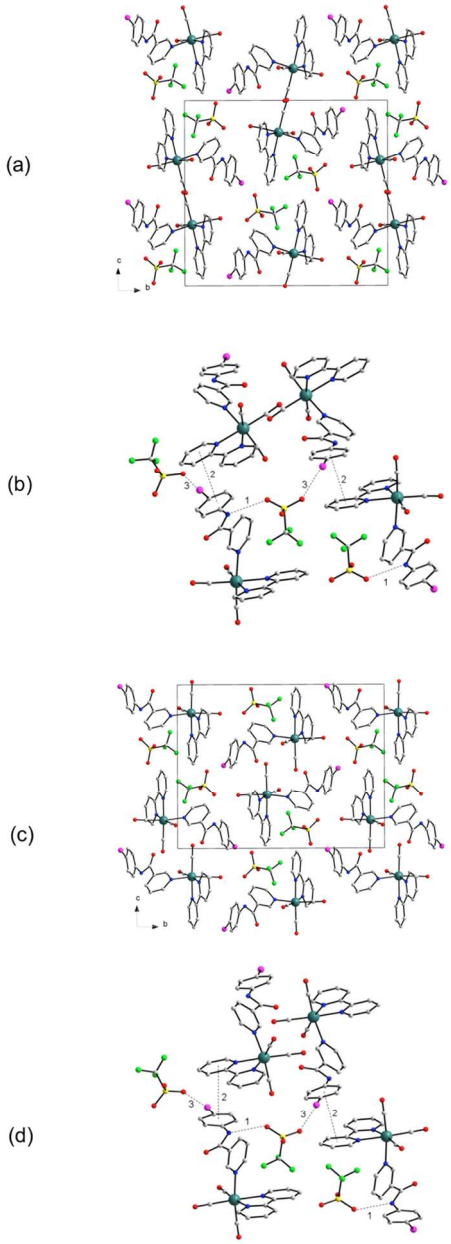

Fig. 8 (a) Crystal packing in the high temperature form of the 4-iodo substituted complex (**Re-*p*-I-HT**) and (b) a segment of the structure. (c) Crystal packing in the low temperature form of the 4-iodo substituted complex (**Re-*p*-I-LT**) and (d) a segment of the structure. Hydrogen atoms have been omitted for clarity.

Table 2 Crystal data collection and refinement details for the *p*-substituted complexes.

	Re-*p*-I-ht	**Re-*p*-I-lt**	**Re-*p*-F**	**Re-*p*-Cl**	**Re-*p*-Br**	**Re-*p*-Me-a**	**Re-*p*-Me-b**
	$C_{26}H_{17}F_3I$ N_4O_7ReS	$C_{26}H_{17}F_3I$ N_4O_7ReS	$C_{26}H_{17}F_4$ N_4O_7ReS	$C_{26}H_{17}ClF_3$ N_4O_7ReS	$C_{26}H_{17}BrF_3$ N_4O_7ReS	$C_{29}H_{24.50}F_3$ $N_5O_{7.50}ReS$	$C_{27}H_{21}F_3$ $N_4O_{7.50}ReS$
FW	899.60	899.60	791.70	808.15	852.61	838.30	796.74
T / K	294(2)	105(2)	150(2)	150(2)	150(2)	110(2)	150(2)
λ / Å	0.71073	0.71073	0.71073	0.71073	0.71073	0.71073	0.71073
System	Monoclinic	Monoclinic	Monoclinic	Triclinic	Monoclinic	Monoclinic	Monoclinic
Space grp	$P2_1/c$	$P2_1/c$	$P2_1/c$	P-1	P21/n	$P2_1/n$	$P2_1/a$
a / Å	9.3050(3)	8.5630(8)	8.3032(3)	10.8109(4)	20.4610(3)	11.4744(8)	12.1162(10)
b / Å	18.7280(8)	20.396(2)	18.0645(5)	11.2437(4)	8.99680(10)	26.9368(19)	27.444(3)
c / Å	17.2820(6)	16.2270(18)	18.8024(7)	13.6707(5)	31.6923(4)	23.6360(14)	19.0654(16)
α / °	90	90	90	109.009(2)	90	90	90
β / °	101.354(2)	94.112(7)	96.9990(10)	91.179(2)	104.2680(10)	96.298(3)	99.666(4)
γ / °	90	90	90	117.018(2)	90	90	90
V / $Å^3$	2952.69(19)	2826.8(5)	2799.22(16)	1371.34(9)	5654.07(13)	7261.4(8)	6249.6(9)
Z	4	4	4	2	8	8	8
$\sigma_{calc}/Mg/m^3$	2.024	2.114	1.879	1.957	2.003	1.534	1.694
Size/ mm^3	0.39×0.30×0.04	0.39×0.30×0.04	0.20×0.01×0.01	0.08×0.06×0.05	0.22×0.15×0.12	0.50×0.02×0.01	0.25×0.08×0.02
Reflections	11154	10313	9272	9088	25612	13694	9833
Unique	6477	5903	5445	6208	13407	7570	5052
R(int)	0.0591	0.0886	0.0724	0.0464	0.0356	0.0720	0.1324
Gof	1.055	1.051	1.042	1.053	1.156	1.079	1.142
R1	0.0607	0.0732	0.0572	0.0590	0.0462	0.0652	0.1207
wR2	0.1403	0.1676	0.0935	0.1118	0.0886	0.1460	0.2300

A description of the crystal structures separately highlighting common structural characteristics will be followed by a discussion of the changes that accompany a phase transition between them.

The high temperature form, Re-*p*-I-HT

In the structure (Fig. 8a) the cation consists of a Re^I coordinated by three carbonyl groups, one bidentate 2,2′-bipyridine ligand and one *N*-(4-iodophenyl)nicotinamide ligand. The coordination geometry of Re is distorted octahedral (N(2)-Re(1) = 2.226(9)Å, N(3)-Re(1) = 2.181(9) Å, N(4)-Re(1) = 2.157(8) Å, C(23)-Re(1) = 1.911(12) Å, C(24)-Re(1) = 1.959(12) Å, C(25)-Re(1) = 1.905(13) Å), the longest contact being to the nicotinamide ligand.

The arrangement of complex cations in the crystal structure creates pockets in the lattice in which triflate anions are accommodated in pairs. The CF_3 and SO_3 groups in the triflate ion are in a staggered conformation. One of the triflate oxygen atoms accepts an amide N-H…O hydrogen bond (labelled *1* in Fig. 8b, with distances H···O = 2.10Å, N···O = 2.94(2) Å, and angle N–H···O = 160.3°). Another triflate oxygen is involved in a short C-I···O interaction (labelled *3* in Fig. 8b, with distance I···O = 3.09(2)Å, angle C-I···O = 170.4(9)°), an example of a halogen bond.[18] The *N*-(4-iodophenyl)nicotinamide ligand is not planar, as indicated by the angle between the planes of the iodophenyl and pyridyl groups (20.2(9)°). π-π type interactions also occur in the structure between the iodophenyl ring of a complex unit and the bipyridine ligand of a neighbouring complex (labelled *2* in Fig. 8b). The centroid-to-centroid separation for the rings involved is 3.86(2) Å (for the major component of the iodophenyl ring) and with an angle of 14.3(9)° between the planes of the rings.

The low temperature form, Re-*p*-I-LT

The coordination geometry of the Re^I ion is closely comparable to that in **Re-*p*-I-HT** (N(2)-Re(1) = 2.237(10)Å, N(3)-Re(1) = 2.181(10) Å, N(4)-Re(1) = 2.162(10) Å, C(23)-Re(1) = 1.931(14) Å, C(24)-Re(1) = 1.935(16) Å, C(25)-Re(1) = 1.923(14) Å). Similarly, one triflate oxygen accepts an N-H···O hydrogen bond (labelled *1* in Fig. 8d, with distances H···O = 2.15Å, N···O = 2.95(2) Å, and angle N–H···O = 151°) and another is involved in a short C-I···O interaction (labelled *3* in Fig. 8d, with distance I···O = 3.21(2)Å, angle C-I···O = 162.7(9)°). The angle between the planes of the iodophenyl and pyridyl groups in the *N*-(4-iodophenyl)nicotinamide ligand is 60(1)°. The centroid-to-centroid distance between the iodophenyl ring and the bipyridine rings involved in π-π interaction (labelled *2* in Fig. 8d) is 4.23(2) Å and the angle between the planes of the rings is 10.8(9)°.

Transformation of Re-*p*-I-HT to Re-*p*-I-LT

The discussion of the crystal structures above and particularly an examination of Fig. 8 reveal a striking similarity between **Re-*p*-I-HT** and **Re-*p*-I-LT**. It is therefore unsurprising that transformation between the two forms has been observed. Indeed, the process takes place in a SC-SC manner and the exact same crystal was used to determine the two structures discussed above. Determination of the unit cell parameters at 20-50K intervals between 340K and 105K indicated that the transformation occurred between 200K and 180K; additional data at 5K intervals within this range narrowed the transition temperature to 180-185K. The cell lengths change as would be expected on transformation of the unit cell (Fig. 9a), but more informative is the sudden change in the cell volume clearly indicating a phase transformation (Fig 9b). Upon cooling the transition results in a

ca 4% decrease in volume with a corresponding increase in density (from 2.024 g/cm^3 to 2.114 g/cm^3). Additionally, recycling between high and low temperatures showed that the process is reversible for this material. This indicates that the free energy curves of the polymorphs cross before the melting points and hence the process is enantiomorphic.

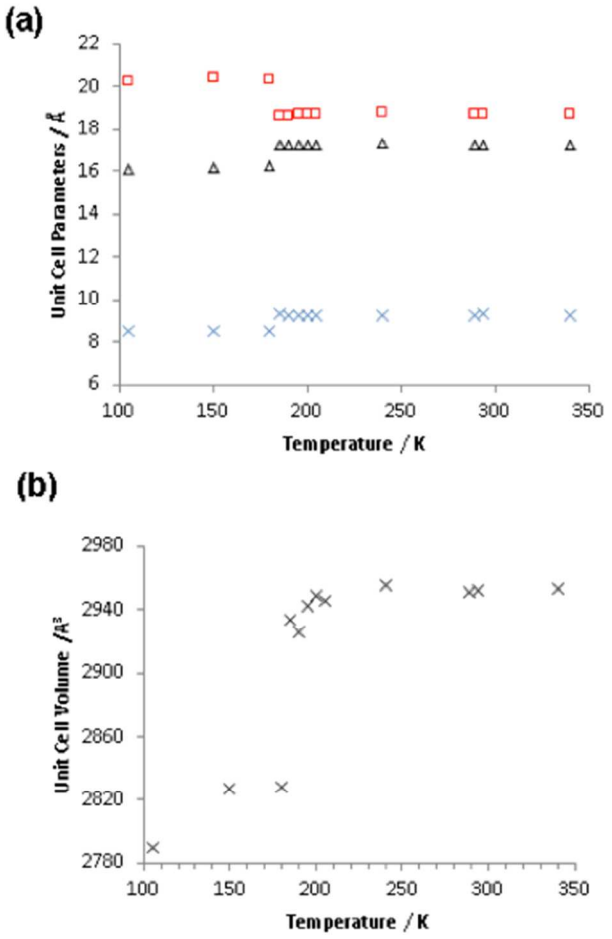

Fig 9. Plot showing the changes in (a) unit cell parameters [blue crosses: *a*-axis, red boxes: *b*-axis, black triangles: *c*-axis], and (b) unit cell volume with temperature.

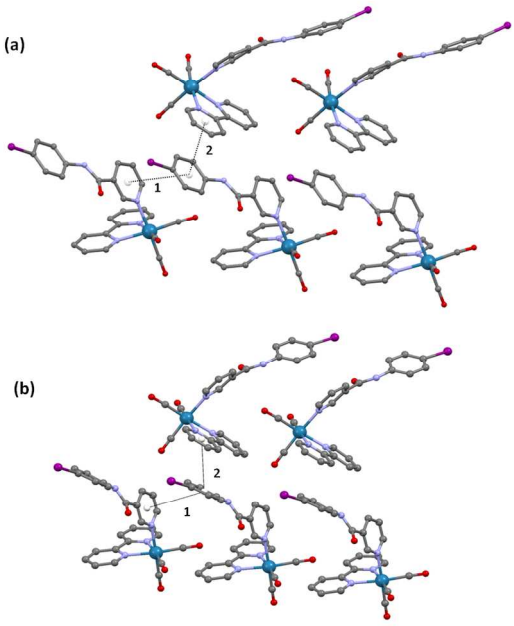

Fig. 10. Segments of the structures of (a) **Re-*p*-I-HT** (major component) and (b) **Re-*p*-I-LT**

The retention of crystal integrity during the phase transformation is an indication: (i) that high steric barriers do not need to be overcome during transformation; or (ii) that the material is flexible enough to accommodate large intracrystal displacements. In the case of **Re-*p*-I-HT** and **Re-*p*-I-LT**, a comparison of the structures indicates similarities consistent with relatively small structural changes. The high temperature unit cell can be roughly transformed to the low temperature cell by the matrix [0.934 0 0.065, 0 1.084 0, 0 0 0.933], but structural transformation involves both molecular reorientation and conformational change. Intramolecularly, as would be expected, the most notable changes involve the more flexible N-(4-iodophenyl)nicotinamide co-ligand. We consider the ligand as consisting of three planes: the pyridyl group, the amide link and the iodobenzene group. On transformation, the orientation of the pyridyl group remains the same on transformation (*i.e.* minimal rotation about the Re-N bond). The amide link rotates by *ca* 6° from the plane of the pyridyl group and the iodobenzene group rotates by a further 34°. The changes in intramolecular geometry are accompanied by relatively small, but significant, adjustments in intermolecular contacts. An example is illustrated in Fig 10. Interactions between the iodobenzene and pyridyl rings of adjacent molecules are labelled ***1*** for **Re-*p*-I-HT**, (Fig 10a) and **Re-*p*-I-LT**. (Fig 10b). For interaction ***1***, an increase in the ring centroid-centroid distance from 4.26(2)Å to 4.52(2) Å is observed on transformation from the high temperature to the low-temperature form. The increase in separation is accompanied by an increase in the angle between the planes of the two rings, from *ca* 20° to *ca* 60°.

Interaction ***2*** in Fig 10 (a) and (b) involves the iodobenzene ring and a bipyridine ring of a neighouring molecule. On transformation from **Re-*p*-I-HT** to **Re-*p*-I-LT** the centroid-

Table 3 Crystal data collection and refinement details for the *o*-substituted complexes.

	Re-*o*-F	**Re-*o*-Br**	**Re-*o*-I**
	$C_{26}H_{17}F_4N_4O_7ReS$	$C_{26}H_{17}BrF_3N_4O_7ReS$	$C_{26}H_{17}F_3IN_4O_7ReS$
FW	791.70	852.61	899.60
T / K	210(2)	150(2)	150(2)
λ / Å	0.71073	0.71073	0.71073
System	Triclinic	Monoclinic	Triclinic
Space grp	P-1	$P2_1/c$	P-1
a / Å	8.5187(3)	12.2430(3)	10.0523(2)
b / Å	11.9891(4)	12.0173(2)	11.6515(4)
c / Å	13.4341(4)	19.2931(4)	13.0988(4)
α / °	77.040(2)	90	69.7400(10)
β / °	89.004(2)	101.5490(10)	78.794(2)
γ / °	84.019(2)	90	82.263(2)
V / $Å^3$	1329.79(8)	2781.08(10)	1408.05(7)
Z	2	4	2
σ_{calc}/Mg/m^3	1.977	2.036	2.122
Size/ mm^3	0.30×0.25×0.03	0.40×0.12×0.12	0.25×0.15×0.10
Reflections	8828	10634	9805
Unique	6007	6359	6443
R(int)	0.0411	0.0345	0.0240
Gof	1.043	1.054	1.046
R1 [I>2σ(I)]	0.0403	0.0410	0.0324
wR2	0.0970	0.0933	0.0716

centroid distance also increases from 3.86(2)Å to 4.23(2) Å but the interplanar angle decreases slightly from 14.3(9) to 10.8(9)°. The short I…O contact (***3*** in Fig. 8b and d) is retained on transformation but lengthens from 3.09(2) Å to 3.21(2) Å.

The phase transition behaviour of **Re-*p*-I** is the result of mutual influence of many factors as there is no single obvious structural feature to which the process can be attributed. Experiments using the rest of the complexes studies did not reveal any transformation over the same temperature range confirming that the enantiotropic transformation of the **Re-*p*-I** is an example of an extremely rare reversible, temperature driven phase transformation for a mononuclear organometallic coordination complex.

Experimental

General Information

All reactions were performed with the use of vacuum line and Schlenk techniques. Reagents were commercial grade and were used without further purification. ^1H and ^{13}C-{^1H} NMR spectra were run on a NMR-FT Bruker 400 and 250 MHz spectrometers and recorded in MeOD or $CDCl_3$. NMR chemical shifts (δ) were determined relative to internal $Si(CH_3)_4$ and are given in ppm. Low-resolution mass spectra were obtained by the staff at Cardiff University. High-resolution mass spectra were carried out by the EPSRC National Mass Spectrometry Service at Swansea University. Infrared spectra were run on a Perkin–Elmer FT-1600 spectrophotometer as $CHCl_3$ solutions. UV-vis studies were performed on a Jasco V-570 spectrophotometer as $CHCl_3$ solutions (*ca.* 10^{-5} M^{-1}). Photophysical data were obtained on a JobinYvon-Horiba Fluorolog spectrometer fitted with a JY TBX picosecond photodetection module as $CHCl_3$ solutions. Emission spectra were uncorrected and excitation spectra were instrument corrected. The pulsed source was a Nano-LED configured for 372 nm output operating at 500 kHz. Luminescence lifetime profiles were obtained using the JobinYvon-Horiba FluoroHub single photon counting module and the data fits yielded the lifetime values using the provided DAS6 deconvolution software.

For crystal structure determination, diffraction data for were collected on a Nonius KappaCCD diffractometer using graphite-monochromated Mo-Kα radiation (λ = 0.71073 Å) and equipped with an Oxford Cryostream cooler. The structures were solved by direct methods and refined using SHELXS-97.[6] Generally, all non-H atoms were refined anisotropically and a riding model was used for hydrogen atoms. Crystallographic data are shown in Tables 2, 3 and S1. The iodobenzene ring in **Re-*p*-I-HT** was refined using a disordered model with major/minor components of occupancy 0.67(2)/0.33(2). The crystals of **Re-*p*-Me-A** and **Re-*p*-Me-B** were thin needles, which gave weak data and low data-to-parameter ratios. Contributory factors include large asymmetric units and disordered solvent molecules necessitating parameter restraints during refinement.

Materials and procedures

Other than *N*-(4-iodophenyl)nicotinamide (*p*-I), each of the ligands [*N*-(p-tolyl)nicotinamide (*p*-Me)[7]; *N*-(2-chlorophenyl) nicotinamide (*o*-Cl)[8]; *N*-(4-bromophenyl)nicotinamide (*p*-Br)[9]; *N*-(4-fluorophenyl)nicotinamide (*p*-F)[7b]; *N*-(2-chlorophenyl) nicotinamide (*o*-Cl)[10]; *N*-(2-bromophenyl)nicotinamide (*o*-Br)[11]; *N*-(2-iodophenyl)nicotinamide (*o*-I)[12]; *N*-(2-fluorophenyl) nicotinamide (*o*-F)[7b,13]] have been previously reported.

A typical synthesis for the ligands: preparation of N-(4-iodophenyl)nicotinamide (p-I)

Nicotinic acid (1.00 g, 8.12 mmol) in $CHCl_3$ (5 ml) was added to a round bottom flask fitted with a condenser and flushed with nitrogen. NEt_3 (1.25 ml, 8.98 mmol) was added, followed by dropwise addition of $SOCl_2$ (2.5 ml, 34.4 mmol). The reaction mixture was stirred under nitrogen at 60 ºC. After 24 h a red solution was afforded, which was dried *in vacuo* (removing excess $SOCl_2$, NEt_3 and HCl) to give nicotinoyl chloride (1.12 g, 97 %) as a red/brown solid which was used without further purification. 4-iodoaniline (2.01 g, 9.18 mmol), Et_2N^iPr (4 ml, 23.0 mmol) and MeCN (10 ml) were added to a round bottom flask containing nicotinoyl chloride (1.12 g, 7.91 mmol) fitted with a condenser, and then flushed with nitrogen. The dark red/brown solution was stirred at 60 ºC. After 24 hrs the solution was dried *in vacuo* (removing MeCN and excess Et_2N^iPr), dissolved in CH_2Cl_2 (15 ml), washed with water (3 × 15 ml), dried over $MgSO_4$, filtered and dried *in vacuo*. Further purification was achieved using column chromatography (Silica:CH_2Cl_2). Unreacted 4-iodoaniline was firstly eluted with CH_2Cl_2, the pure product eluted with CH_2Cl_2/MeOH (95:5) to give *N*-(4-iodophenyl)nicotinamide (yield: 1.95 g, 74 %) as a light brown solid. ^1H NMR ($CDCl_3$, 400 MHz, 298 K) δ_H: 7.38 (3H, m), 7.63 (2H, d, $^3J_{HH}$ = 8.8 Hz), 7.86 (1H, s, N*H*), 8.13 (1H, m), 8.72 (1H, d, $^3J_{HH}$ = 3.2 Hz), 9.01 (1H, s) ppm. IR ($CHCl_3$) ν_{max}: 1685, 1590, 1514, 1488 cm^{-1}. EIMS *m/z*: found 324.0 $[M]^+$.

General method for the synthesis of the complexes

Typically *fac*-[$Re(CO)_3$(2,2′-bipyridine)(CH_3CN)][OTf] (0.0993

mmol) was added to a round bottom flask fitted with a condenser. The *N*-(halophenyl)nicotinamide (0.111 mmol) and chloroform (10 mL) were added to the reaction flask and flushed with nitrogen. The reaction was heated at 60 ºC for 24 h. A yellow solution was afforded; solvent was then removed and the residue dried *in vacuo*. The title product was afforded in powdered form *via* re-precipitation from $CHCl_3$/ Et_2O to give the title complex in each case.

Synthesis of fac-[Re(CO)$_3$(2,2´-bipyridine)(N-(4-iodophenyl)nicotinamide)][OTf] (Re-p-I)
Obtained as a yellow solid (Yield: 89 %). ^{1}H NMR ($CDCl_3$, 250 MHz, 298 K) δ_H: 7.30 (1H, m), 7.40 (2H, d, $^3J_{HH}$ = 8.8 Hz), 7.51 (2H, d, $^3J_{HH}$ = 8.0 Hz), 7.59 (1H, d, $^3J_{HH}$ = 8.3 Hz), 7.69 (2H, m), 8.15 (2H, m), 8.21 (1H, d, $^3J_{HH}$ = 5.4 Hz), 8.26 (1H, d, $^3J_{HH}$ = 8.0 Hz), 8.33 (3H, m, Ar*H*, N*H*), 9.10 (2H, d, $^3J_{HH}$ = 6.3 Hz), 9.67 (1H, s) ppm. IR ($CHCl_3$) ν_{max}: 2037, 1933, 1680 cm^{-1}. UV-vis (CH_3Cl) λ_{max} (ε = M^{-1} cm^{-1}): 251 (30400), 279 (30800), 369 sh (10300) nm. Emission ($CHCl_3$) λ_{em} (τ / ns): 545 (348) nm. ESMS *m/z*: calculated 750.4, found 750.9 [M - OTf]$^+$; HRMS *m/z*: calculated 748.9819, found 748.9822 [$C_{25}H_{17}IN_4O_4{}^{185}Re$]$^+$.

Synthesis of fac-[Re(CO)$_3$(2,2´-bipyridine)(N-(2-iodophenyl)nicotinamide)][OTf] (Re-o-I)
Obtained as a yellow solid (Yield: 89 %). ^{1}H NMR ($CDCl_3$, 250 MHz, 298 K) δ_H: 6.91 (1H, d, $^3J_{HH}$ = 8.9 Hz), 7.31 (1H, d), 7.49 (1H, d, $^3J_{HH}$ = 8.9 Hz), 7.6-7.9 (3H, m), 7.9-8.3 (4H, m), 8.4-8.6 (3H, m), 8.71 (1H, br s), 9.0-9.2 (2H, overlapping m) ppm. IR ($CHCl_3$) ν_{max}: 2026, 1928, 1900, 1681 cm^{-1}. UV-vis (CH_3Cl) λ_{max} (ε = M^{-1} cm^{-1}): 250 (25600), 273 (23600), 370 sh (6300) nm. Emission ($CHCl_3$) λ_{em} (τ / ns): 542 (334) nm. ESMS *m/z*: calculated 751.0, found 751.0 [M - OTf]$^+$; HRMS: *m/z* calculated 748.9819, found 748.9817 [$C_{25}H_{17}IN_4O_4{}^{185}Re$]$^+$.

Synthesis of fac-[Re(CO)$_3$(2,2´-bipyridine)(N-(4-fluorophenyl)nicotinamide)][OTf] (Re-p-F)
Obtained as a yellow solid (Yield: 81 %). ^{1}H NMR ($CDCl_3$, 250 MHz, 298 K) δ_H: 7.30 (1H, m), 7.40 (2H, d, $^3J_{HH}$ = 8.1 Hz), 7.51 (2H, d, $^3J_{HH}$ = 8.0 Hz), 7.59 (1H, d, $^3J_{HH}$ = 7.9 Hz), 7.69 (2H, m), 8.15 (2H, m), 8.21 (1H, d, $^3J_{HH}$ = 5.4 Hz), 8.26 (1H, d, $^3J_{HH}$ = 8.0 Hz), 8.30-8.37 (3H, m), 9.10 (2H, d, $^3J_{HH}$ = 6.3 Hz), 9.67 (1H, s) ppm. IR ($CHCl_3$) ν_{max}: 2026, 1928, 1899, 1682 cm^{-1}. UV-vis (CH_3Cl) λ_{max} (ε = M^{-1} cm^{-1}): 244 (11050), 292 (10000), 396 (1600) nm. Emission ($CHCl_3$) λ_{em} (τ / ns): 549 (324) nm. ESMS *m/z*: calculated 643.1, found 643.1 [M - OTf]$^+$; HRMS *m/z*: calculated 641.0758, found 641.0751 [$C_{25}H_{17}O_4N_4F^{185}Re$]$^+$.

Synthesis of fac-[Re(CO)$_3$(2,2´-bipyridine)(N-(2-fluorophenyl)nicotinamide)][OTf] (Re-o-F)
Obtained as a yellow solid (Yield: 85 %). ^{1}H NMR ($CDCl_3$, 250 MHz, 298 K) δ_H: 7.03 (2H, d, $^3J_{HH}$ = 7.92 Hz), 7.33 (1H, br s), 7.47 (2H, d, $^3J_{HH}$ = 8. 0 Hz), 7.69 (2H, br s), 8.1-8.5 (7H, m), 9.03 (1H, d, $^3J_{HH}$ = 5.1 Hz), 9.11 (2H, d, $^3J_{HH}$ = 5.1 Hz) ppm. IR ($CHCl_3$) ν_{max}: 2026, 1928, 1900, 1681 cm^{-1}. UV-vis (CH_3CN) λ_{max} (ε = M^{-1} cm^{-1}): 249 (28200), 275 (28600), 358 sh (4600) nm. Emission ($CHCl_3$) λ_{em} (τ / ns): 542 (341) nm. ESMS (ES) *m/z*: calculated 643.1, found 643.1 [M - OTf]$^+$; HRMS *m/z*: calculated 641.0758, found 641.0754 [$C_{25}H_{17}O_4N_4F^{185}Re$]$^+$.

Synthesis of fac-[Re(CO)$_3$(2,2´-bipyridine)(N-(4-chlorophenyl)nicotinamide)][OTf] (Re-p-Cl)
Obtained as a yellow solid (Yield: 65 %). ^{1}H NMR ($CDCl_3$, 250 MHz, 298 K) δ_H: 7.14 (2H, d, $^3J_{HH}$ = 8.1 Hz), 7.51 (2H, d, $^3J_{HH}$ = 8.10 Hz), 7.60-7.75 (3H, m), 8.10-8.40 (8H, m), 9.11 (2H, d, $^3J_{HH}$ = 6.3 Hz), 9.69 (1H, s) ppm. IR ($CHCl_3$) ν_{max}: 2037, 1933, 1680 cm^{-1}. UV-vis (CH_3Cl) λ_{max} (ε = M^{-1} cm^{-1}): 245 (17800), 278 (18400), 321 (7500), 365 sh (2600) nm. Emission ($CHCl_3$) λ_{em}: 538 nm. ESMS *m/z*: calculated 659.1, found 659.1 [M - OTf]$^+$. HRMS *m/z*: calculated 657.0462, found 657.0462 [$C_{25}H_{17}O_4N_4Cl^{185}Re$]$^+$.

Synthesis of fac-[Re(CO)$_3$(2,2´-bipyridine)(N-(2-chlorophenyl)nicotinamide)][OTf] (Re-o-Cl)
Obtained as a yellow solid (Yield: 71 %). ^{1}H NMR ($CDCl_3$, 250 MHz, 298 K) δ_H: 6.9-7.2 (2H, m), 7.4-7.6 (2H, overlapping m), 7.59 (1H, d, $^3J_{HH}$ = 8.8 Hz), 7.69 (2H, m), 7.9-8.2 (5H, m), 8.7-8.9 (2H, m), 9.02 (2H, d, $^3J_{HH}$ = 6.3 Hz), 9.41 (1H, br s) ppm. IR ($CHCl_3$) ν_{max}: 2038, 1933, 1680 cm^{-1}. UV-vis (CH_3CN) λ_{max} (ε = M^{-1} cm^{-1}): 247 (26100), 294 (27400), 392 (4400) nm. Emission ($CHCl_3$) λ_{em} (τ / ns): 548 (333) nm. ESMS *m/z*: calculated 659.1, found 659.0 [M - OTf]$^+$. HRMS *m/z*: calculated 657.0462, found 657.0457 [$C_{25}H_{17}O_4N_4F^{185}Re$]$^+$.

Synthesis of fac-[Re(CO)$_3$(2,2´-bipyridine)(N-(4-bromophenyl)nicotinamide)][OTf] (Re-p-Br)
Obtained as a yellow solid (Yield: 84 %). ^{1}H NMR ($CDCl_3$, 250 MHz, 298 K) δ_H: 7.28 (2H, d, $^3J_{HH}$ = 7.9 Hz), 7.51 (2H, d, $^3J_{HH}$ = 8.10 Hz), 7.60-7.75 (3H, m), 8.10-8.40 (8H, m), 8.96 (1H, d, $^3J_{HH}$ = 8.7 Hz), 9.11 (2H, d, $^3J_{HH}$ = 6.3 Hz), 9.61 (1H, s) ppm.IR ($CHCl_3$) ν_{max}: 2037, 1933, 1680 cm^{-1}. UV-vis (CH_3CN) λ_{max} (ε = M^{-1} cm^{-1}): 248 (24200), 283 (25300), 363 sh (5300) nm. Emission ($CHCl_3$) λ_{em} (τ / ns): 542 (359) nm. ESMS *m/z*: calculated 703.0, found 703.0 [M - OTf]$^+$; HRMS *m/z*: calculated 700.9957, found 700.9956 [$C_{25}H_{17}O_4N_4Br^{185}Re$]$^+$.

Synthesis of fac-[Re(CO)$_3$(2,2´-bipyridine)(N-(2-bromophenyl)nicotinamide)][OTf] (Re-o-Br)
Obtained as a yellow solid (Yield: 73 %). ^{1}H NMR ($CDCl_3$, 250 MHz, 298 K) δ_H: 6.94 (1H, d, $^3J_{HH}$ = 8.3 Hz), 7.32 (1H, d), 7.49 (1H, d, $^3J_{HH}$ = 7.7 Hz), 7.6-8.3 (7H, overlapping m), 8.40-8.60 (3H, m), 8.71 (1H, br s), 9.11 (2H, d, $^3J_{HH}$ = 8.2 Hz) ppm. IR ($CHCl_3$) ν_{max}: 2037, 1929 cm^{-1}. UV-vis ($CHCl_3$) λ_{max} (ε = M^{-1} cm^{-1}): 250 (29600), 273 (29600), 322 (16300), 358 sh (6600) nm. Emission ($CHCl_3$) λ_{em} (τ / ns): 542 (351) nm. ESMS *m/z*: calculated 703.0, found 703.0 [M - OTf]$^+$; HRMS *m/z*: calculated 700.9957, found 700.9956 [$C_{25}H_{17}O_4N_4Br^{185}Re$]$^+$.

Synthesis of fac-[Re(CO)$_3$(2,2´-bipyridine)(N-(p-tolyl)nicotinamide)][OTf] (Re-p-Me)
Obtained as a yellow solid (Yield: 74 %). ^{1}H NMR ($CDCl_3$, 250 MHz, 298 K) δ_H: 2.23 (3H, s, CH_3), 7.03 (2H, d, $^3J_{HH}$ = 7.9 Hz), 7.28 (1H, br s), 7.47 (2H, d, $^3J_{HH}$ = 8.5 Hz), 7.67 (2H, t, $^3J_{HH}$ = 6.55 Hz), 8.1-8.4 (8H, m), 9.08 (2H, d, $^3J_{HH}$ = 5.1 Hz), 9.44 (1H, br s) ppm. IR ($CHCl_3$) ν_{max}: 2036, 1939 cm^{-1}. UV-vis ($CHCl_3$) λ_{max} (ε = M^{-1} cm^{-1}): 247 (25900), 277 (26200), 322 (15200), 362 sh (6700) nm. Emission ($CHCl_3$) λ_{em} (τ / ns): 543 (339) nm. ESMS *m/z*: calculated 639.1, found 639.1 [M - OTf]$^+$. HRMS *m/z*: calculated 637.1009, found 637.1006 [$C_{26}H_{20}N_4O_4{}^{185}Re$]$^+$.

Conclusions

A systematic structural survey of a series of monometallic complexes (twelve examples in total) based on the core formulation *fac*-[Re(CO)$_3$bipy(L)](OTf) revealed that one of the species, **Re-*p*-I**, with an iodine-substituted axial co-ligand, possesses an extremely rare, temperature driven phase transformation. This transformation process is reversible and proceeds in a single-crystal to single-crystal manner. Somewhat surprisingly, this species was found to be anomolous within the series of closely related molecular analogues.

Clearly, the other crystalline materials obtained in this study do not undergo transformation. However, the premise for a meaningful detailed discussion on the effect of systematic chemical modification is the existence of isomorphism. No isomorphism was found between the derivatives discussed in this study. It is therefore not possible to predict how the other derivatives would behave were alternative crystal structures to be obtained.

It is also noteworthy that apart from the two forms of **Re-*p*-I**, polymorphism was not observed for any other species in the series, further exemplifying the unique behaviour of **Re-*p*-I** in this study. Of all the structures, only **Re-*p*-Me** is solvated and two solvates have been obtained which, although not polymorphs, have many similar structural features.

Acknowledgements

We thank Cardiff University and EPSRC for financial support and the staff of the NMSCC at Swansea University.

Notes and references

[a] *School of Chemistry, Cardiff University, Park Place, Cardiff, UK. Fax: (+)44 (0)29 208 74030; Tel: (+)44 (0)29 208 74023; E-mail: popesj@cardiff.ac.uk; kariukib@cardiff.ac.uk*

† Electronic Supplementary Information (ESI) available: [cif files and structural characterisation of the ligands]. See DOI: 10.1039/b000000x/

‡ CCDC 893632-893645 contain the supplementary crystallographic data for this paper. These data can be obtained free of charge from The Cambridge Crystallographic Data Centre *via* www.ccdc.cam.ac.uk/data_request/cif.

(1) G. M. J. Schmidt, *Pure and Appl. Chem.,* 1971, **27**, 647.

(2) C. R. Theocharis, W. Jones in Organic Solid State Chemistry (Ed.: G. R. Desiraju), Elsevier, **1987**, chap. 2, pp. 47

(3) (a) J. Sun, F. Dai, W. Yuan, W. Bi, X. Zhao, W. Sun, D. Sun, *Angew. Chem. Int. Ed.,* 2011, **50**, 7061; (b) O. V. Zenkina, E. C. Keske, R. Wang, C. M. Crudden, *Angew. Chem. Int. Ed.,* 2011, **50**, 8100; (c) A. Igashira-Kamiyama, N. Matsushita, R. Lee, K. Tsuge, T. Konno, *Bull. Chem. Soc. Jpn.,* 2012, **6**, 706; (d) M. Gustafsson, J. Su, H. Yue, Q. Yao, X. Zou, *Cryst. Growth Des.,* 2012, **12**, 3243; (e) J. Li, L. Li, H. Hou, Y. Fan, *Cryst. Growth Des.,* 2009, **9**, 4504; (f) Y-M. Song, F. Luo, M-B. Luo, Z-W. Liao, G-M. Sun, X-Z. Tian, Y. Zhu, Z-J. Yuan, S-J. Liu, W-Y. Xu, X-F. Feng, *Chem. Commun.,* 2012, **48**, 1006; (g) H. Sato, R. Matsuda, M. H. Mir, S. Kitagawa, *Chem. Commun.,* 2012, **48**, 7919; (h) Y.-C. He, J. Yang, G.-C. Yang, W.-Q. Kan, J.-F. Ma, *Chem. Commun.,* 2012, **48**, 7859; (i) X.-J. Yang, S.-S. Bao, T. Zheng, L.-M. Zheng, *Chem. Commun.,* 2012, **48**, 6565; (j) L. Zorina, S. Simonov, E. Canadell, R. Shibaeva, *Crystals,* 2012, **2**, 627; (k) Y.-Q. Lan, H.-L. Jiang, S.-L. Li, Q. Xu, *Inorg. Chem.,* 2012, **51**, 7484; (l) D. L. Reger, J. J. Horger, M. D. Smith, G. J. Long, F. Grandjean, *Inorg. Chem.,* 2011, **50**, 686; (m) H.-X. Zhang, F. Wang, Y.-X. Tan, Y. Kang, J. Zhang, *J. Mater. Chem.,* 2012, **22**, 16288; (n) S. C. Sahoo, T. Kundu, R. Banerjee, *J. Am. Chem. Soc.,* 2011, **133**, 17950; (o) J. Tian, L.V. Saraf, B. Schwenzer, S. M. Taylor, E.K. Brechin, J. Liu, S.J. Dalgarno, P.K. Thallapally, *J. Am. Chem. Soc.* 2012, **134**, 9581; (p) M. R. Montney, R.M. Supkowski, R. J. Staples, R. L. LaDuca, *J. Sol. Stat. Chem.,* 2009, **182**, 8; (q) Z. Huang, P. S. White, M. Brookhart, *Nature,* 2010, **465**, 598; (r) P. Spearman, S. Tavazzi, L. Silvestri, A. Burini, A. Borghesi, P. Mercandelli, M. Panigati, G. D'Alfonso, A. Sironi, L. De Cola, *Proceedings of SPIE,* 2012, *8435* (Organic Photonics V), 84352D-84352-10; (s) C. G. Bezzu, M. Helliwell, J. E. Warren, D. R. Allan, N. B. McKeown, *Science,* 2010, **327**, 1627; (t) A. Lennartson, M. Hakansson, S. Jagner, *New J. Chem.,* 2007, **31**, 344; (u) S. Supriya, S. K. Das, *J. Am. Chem. Soc.,* 2007, **129**, 3464.

(4)(a) M. D. Meijer, R. J. M. K. Gebbink, G. Van Koten, *Perspect. Supramol. Chem.,* 2003, **7**, 375; (b) G. Desiraju, *Crystal Engineering: The Design of Organic Solids*, Elsevier, Amsterdam, 1989.

(5) R. T. Macaluso, S. Nakatsuji, K. Kuga, E. L. Thomas, Y. Machida, Y. Maeno, Z. Fisk, J. Y. Chan, *Chem. Mater.,* 2007, **19**, 1918.

(6) G. M. Sheldrick, *Acta Crystallogr., Sect.A: Fundam. Crystallogr.* 2008, **64**, 112.

(7)(a) J. Chen, G. Ling, Z. Yu, S. Wu, X. Zhao, X. Wu, S. Lu, *Adv. Synth. Catal.,* 2004, **346**, 1267; (b) P. M. Harrington, *Heterocycles,* 1993, **35**, 683.

(8)(a) C-Y. Shi, E-J. Gao, S. Ma, M-L. Wang, Q-T. Liu, *Bioorg. Med. Chem. Lett.,* 2010, **20**, 7250; (b) S. Ushida, *Chem. Lett.,* 1989, 59.

(9)(a) R. W. Dunlop, J. Duncan, G. Ayrey, *Pestic. Sci.,* 1980, **11**, 53; (b) J. Mirek, J. Dydula, *J. Chromatogr*., 1979, **171**, 462.

(10) Y-T. Park, C-H. Jung, K-W. Kim, H-S. Kim, *J. Org. Chem.,* 1999, **64**, 8546.

(11) G. Evindar, R. A. Batey, *J. Org. Chem.,* 2006, **71**, 1802.

(12) L. Basolo, E. M. Beccalli, E. Borsini, G. Broggini, *Tetrahedron* 2009, **65**, 3486.

(13) R. U. Kadam, J. Tavares, V. M. Kiran, A. Cordeiro, A. Ouaissi, N. Roy, *Chem. Bio. Drug Des.,* 2008, **71**, 501.

(14) A. Dey, G. R. Desiraju, *CrystEngComm*., 2004, **6**, 642.

(15)(a) M. R. Edwards, W. Jones, W. D. S. Motherwell, G. P. Shields, *Mol. Cryst. Liq. Cryst.,* 2001, **356**, 337; (b) S. Ebenezer, P. T. Muthiah, R. J. Butcher, *Cryst. Growth Des.,* 2011, **11**, 3579.

(16)(a) F. L. Thorp-Greenwood, M. P. Coogan, A. J. Hallett, R. H. Laye, S. J. A. Pope, *J. Organomet. Chem.,* 2009, **694**, 1400; (b) L. A. Mullice, S. J. A. Pope, *Dalton Trans.,* 2010, **39**, 5908; (c) J. E. Jones, B. M. Kariuki, B. D. Ward, S. J. A. Pope, *Dalton Trans.,* 2011, **40**, 3498; (d) M. P. Coogan, V. Fernandez-Moreira, J. B. Hess, S. J. A. Pope, C. Williams, *New J. Chem.,* 2009, **33**, 1094; (e) A. J. Hallett, P. Christian, J. E. Jones, S. J. A. Pope, *Chem. Commun.,* 2009, 4278; (f) R.O. Bonello, I.R. Morgan, L.E.J. Jones, B.M. Kariuki, I.A. Fallis, S.J.A. Pope, *J. Organomet. Chem*., 2014, **749**, 150; (g) R.G. Balasingham, F.L. Thorp-Greenwood, C.F. Williams, M.P. Coogan, S.J.A. Pope, *Inorg. Chem*., 2012, **51**, 1419; (h) A.J. Hallett, S.J.A. Pope, *Inorg. Chem. Commun*., 2011, **14**, 1606.

(17)(a) M. Wrighton, D. L. Morse, *J. Am. Chem. Soc.,* 1974, **95**, 998; (b) L. Sacksteder, A. P. Zipp, E. A. Brown, J. Streich, J. N. Demas, B. A. DeGraff, *Inorg. Chem.,* 1990, **29**, 4335; (c) L. A. Worl, R. Duessing, P. Chen, L. Della Ciana, T. J. Meyer, *J. Chem. Soc., Dalton Trans.,* 1991, 849.

(18) P. Metrangolo, H. Neukirch, T. Pilati, G. Resnati, *Acc. Chem. Res.,* 2005, **38**, 386.